Heliophysics Science by the NLSI LUNAR Team:

Solar Radio Astronomy, Particle Acceleration, & Interplanetary Dust

Science from the Moon undertaken by the

NASA Lunar Science Institute LUNAR[1] Team

Director: Dr. Jack Burns, University of Colorado Boulder

Deputy Director: Dr. Joseph Lazio, JPL

Authors: Dr. Robert MacDowall, NASA/GSFC

Dr. Justin Kasper, Harvard-Smithsonian CfA

LUNAR Overview

Our Moon is a unique platform from which to conduct measurements of gravitation, the Sun, the lunar ionosphere and interior, and the very early Universe. The Lunar University Network for Astrophysics Research (LUNAR) is addressing the question of how the Moon can be used as a platform to advance important goals in astrophysics, heliophysics, lunar science, the physical sciences, and exploration science. There are three primary areas of research:

(1) Gravitational Physics and Lunar Structure: An enduring legacy of Apollo is the Lunar Laser Ranging (LLR) package that has been used to test alternate theories to General Relativity and to uniquely constrain the nature of the lunar core. The LLR key project of the LUNAR team is addressing the design, fabrication and emplacement of the next generation of retro-reflectors for the Moon. These improvements will make laser ranging measurements a hundred times more accurate. Initial work indicates that currently available retroreflecting cubes are very likely to perform well when scaled up to the size required for new lunar retroreflectors. In addition, efforts are focusing on developing in-house capabilities for assembling more stable and sophisticated hollow cubes using a technique known as hydroxide-catalysis bonding.

(2) Heliophysics: Heliophysics team members are engaged in the general challenge of understanding the deep-space radiation environment, both to understand the fundamental physics of particle acceleration and to enable human exploration. The high temperature solar corona produces the supersonic solar wind that creates a magnetic bubble around our solar system called the heliosphere. Over the course of the eleven-year cycle of solar activity the heliosphere changes. These changes include violent solar flares and coronal mass ejections, which can affect communications, navigation, and human safety. The LUNAR team is examining the role of low-frequency radio observations of the heliosphere from the surface of the Moon in determining how the Sun accelerates particles to high energy. This includes using existing radio observations from the two STEREO spacecraft and optimizing the design of a lunar surface solar imaging radio array at frequencies <10 MHz. Additional work includes developing the ability of radio receivers in space to study dust, and the use of imaging at low frequencies to detect unknown radio transients. .

(3) Low Frequency Cosmology and Astrophysics: After the Big Bang, there was an interval of perhaps a few hundred million years known as the "Dark Ages," before the formation of the first stars and galaxies. Probing the evolution of the Universe during the Dark Ages and as the first stars form is possible using a low radio frequency telescope on or in orbit above the farside of the Moon. The team has developed a model of expected spectral features in the observable all-sky radio signal below 100 MHz which correspond to key moments in history of the Universe. The LUNAR team (in collaboration with other NLSI members) is examining the scientific case for future radio telescopes in lunar orbit or on the lunar surface. Technology development is underway for (1) an antenna in lunar orbit to observe the all-sky signal and (2) a lunar radio array with a large number of antennas, for which high sensitivity and low mass are key requirements. Such low frequency telescopes will also be used to measure the lunar ionosphere and to probe magnetospheric radio missions from exoplanets around other stars.

1. Solar Radio Burst Imaging from the Lunar Surface – Remote Detection of Particle Acceleration

Project Leaders: Dr. Justin Kasper, Harvard-Smithsonian Center for Astrophysics
Dr. Robert MacDowall, NASA Goddard Space Flight Center

a. *Introduction*

We can detect the intense radio bursts produced by energetic electrons as they are accelerated close to the Sun, but no one has been able to image this emission more than a few solar radii above the surface of the Sun. Imaging the emission would show us where acceleration is occurring, immediately allowing us to determine the coronal conditions that lead to efficient particle acceleration, and to forecast if radiation is likely to reach Earth and explorers in space. Almost all of this radio emission is at frequencies lower than the terrestrial ionospheric cutoff, preventing observation from the ground. To date, radio astronomy-capable space missions consist of one or a few satellites, typically far from each other, which measure total power from the radio sources, but cannot produce images with useful angular resolution. To produce such images, we require arrays of antennas distributed over many wavelengths (hundreds of meters to kilometers) to permit aperture synthesis imaging. Such arrays could be readily implemented with antennas placed on the lunar surface. If such an array were in place by 2022, it would provide context for observations during Solar Probe Plus perihelion passes. Studies of interplanetary and lunar dust could also be accomplished by measuring the voltages due to dust impacts on the lunar antennas.

b. *Scientific goals*

High-energy particle acceleration occurs in diverse astrophysical environments including the Sun and other stars, supernovae, black holes, and quasars. A fundamental problem is understanding the mechanisms and sites of this acceleration, in particular the roles of shock waves and magnetic reconnection. Within the inner heliosphere, solar flares and shocks driven by coronal mass ejections (CMEs) are efficient particle accelerators.

Low frequency observations provide an excellent remote diagnostic because electrons accelerated in these regions can produce intense radio bursts. The intensities of these bursts make them easy to detect, as well as providing information about the acceleration regions. The radio burst mechanisms discussed here occur at the local plasma frequency, $f_p \approx 9\ n_e^{1/2}$ kHz, or its harmonics, where n_e is the electron density in cm^{-3}. With a model for n_e, f_p can be converted into a height above the corona, and changing f_p can be converted into radial speed. Observations by widely-separated spacecraft permit triangulation.

Solar radio bursts are one of the primary remote signatures of electron acceleration in the inner heliosphere and our focus is on two emission processes, referred to as Type II and Type III radio bursts. Type II bursts originate from suprathermal electrons (E > 100 eV) produced at shocks. These shocks generally are produced by CMEs as they expand into the heliosphere with Mach numbers greater than unity. Emission from a Type II burst drops slowly in frequency as the shock moves away from the Sun into lower density regions at speeds of ~400–2000 km s^{-1}. Type III bursts are generated by fast (2–20 keV) electrons from magnetic reconnection, typically due to solar flares. As the fast electrons escape at a

significant fraction of the speed of light into the heliosphere open along magnetic field lines, they produce emission that drops rapidly in frequency (see Figure 1).

Electron densities in the inner heliosphere yield relevant frequencies below ~10 MHz. Observations must be conducted from space because the ionosphere is opaque in this frequency range. Figure 1 illustrates the active low-frequency radio environment in space, including terrestrial radio frequency interference (RFI), as seen by the WAVES instrument on the Wind spacecraft (Bougeret et al. 1995). Solar radio observations from the near side of the moon would necessarily be made in the gaps between the RFI.
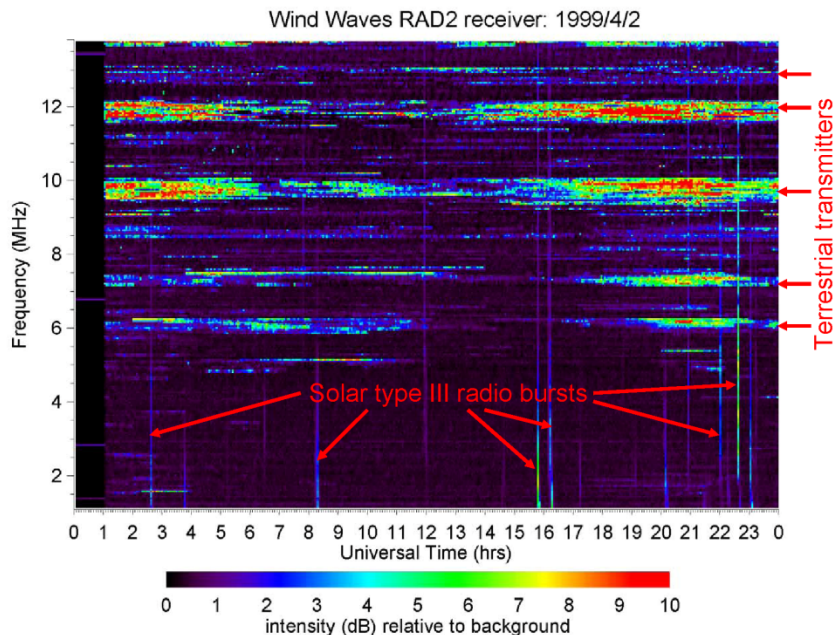

Fig. 1 - Observed low-frequency radio environment when the Wind spacecraft was near the moon. The 24-hr dynamic spectrum covers 1–14 MHz, with the intensity on a logarithmic color scale.

c. *Acceleration at Shocks*

Observations of CMEs near Earth suggest electron acceleration generally occurs where the shock normal is perpendicular to the magnetic field (Bale et al. 1999), similar to acceleration at planetary bow shocks and other astrophysical sites. This geometry may be unusual in the corona, where the magnetic field is largely radial, as shown schematically in Figure 2a. There, the shock at the front of a CME generally has a quasi-parallel geometry (Q-∥). Acceleration along the flanks of the CME, where the magnetic field-shock normal is quasi-perpendicular (Q-⊥) would seem to be a more likely location for the electron acceleration and Type II emission. The radio array needs ~2° resolution to localize these acceleration site(s), yielding the preferred geometry (Q-∥ vs. Q-⊥) for radio emission around CMEs.

Observations at 1–14 MHz made with the Wind spacecraft showed that complex Type III-L bursts are highly correlated with CMEs and intense (proton) solar energetic particle (SEP) events observed at 1 AU (Cane et al. 2002; Lara et al. 2003, MacDowall et al. 2003). While the association between Type III-L bursts, proton SEP events, and CMEs is now secure, the electron acceleration mechanism remains poorly understood. Two competing sites for the acceleration have been suggested: at shocks in front of the CME or in reconnection regions behind the CME; see Figure 2b. For typical limb CMEs, the angular separation of the leading edge of the shock and the hypothesized reconnection region behind the CME is approximately 1.5° when the CME shock is 3–4 $R_\odot$ from the Sun.
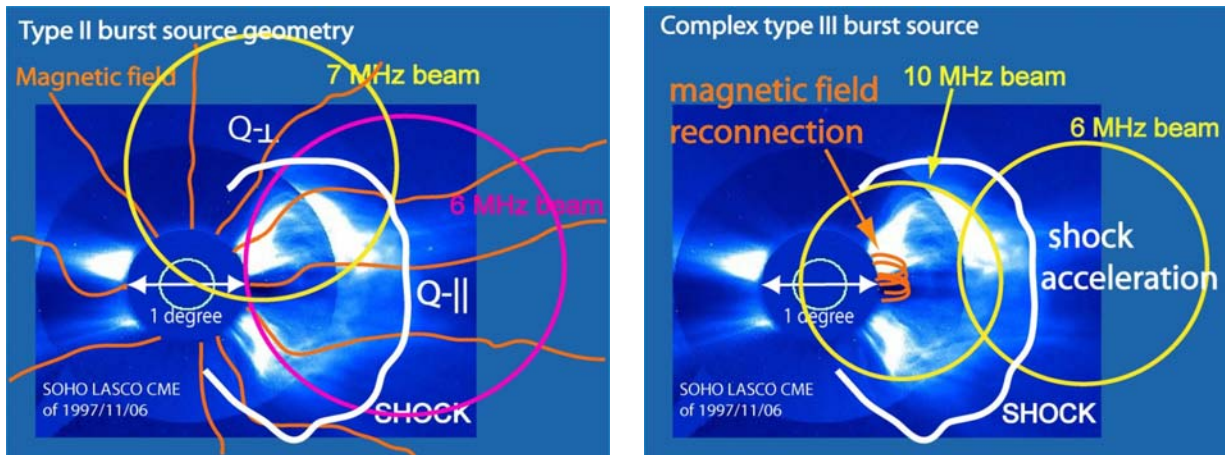
Fig. 2a – (Left) Where on the shock does electron acceleration occur, yielding type II radio emission?
Fig. 2b - (Right) Are complex type III-L bursts produced by shock acceleration or reconnection?

d. *CME Interactions and Solar Energetic Particle (SEP) Event Intensity*

Unusually intense radio emission can occur when successive CMEs leave the Sun within 24 hours, as if CME interaction produces enhanced particle acceleration (Gopalswamy et al. 2001, 2002). Statistically associated with intense SEP events (Gopalswamy et al. 2004), this enhanced emission could result from more efficient acceleration due to changes in field topology, enhanced turbulence, or direct interaction of the CMEs. Lack of radio imaging makes it difficult to determine the nature of the interaction. Images with ~2 degree resolution would give Type II locations and permit identification of the causal mechanism and the relation to intense SEPs.

e. *Relevance to Solar Probe Plus (SPP)*

The ROLSS mission would image radio sources in the volume from ~2 to 10 solar radii, corresponding to the region sunward of SPP perihelion passes. Remote radio imaging would give locations of electron acceleration related to solar flaring and (fast) CMEs in the environment of SPP, yielding a context for understanding solar energetic particle acceleration - one of SPP's key goals. They would also provide relative timing of events and indicate the outward propagation altitude and direction of the events. Such observations would provide a large scale perspective, complementary to those of the all-sky image, aiding to determine the structure and dynamics of the magnetic fields at the sources of the fast and slow solar wind, another SPP goal. Orbits of Solar Probe Plus are shown in Figure 3.
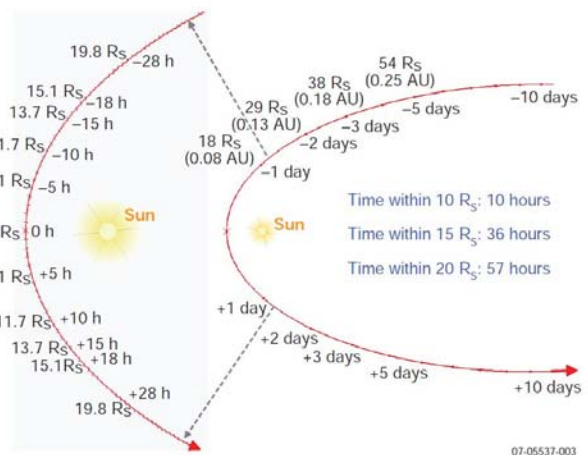
Fig. 3 – The planned closest perihelion for SPP is 9.4 AU. At that distance from the sun (and outward) the emission frequencies of radio bursts are below the terrestrial ionospheric cutoff.

5

f. Astronaut safety from Space Weather

Heliophysics science has been tightly coupled with exploration since the beginning of the space program, as scientists work to both understand the physics connecting the Sun and the Earth to the rest of the solar system, and to develop predictive capabilities that enable operational planning for lunar, deep space, and eventually Mars missions. Renewed robotic and human exploration of the moon creates opportunities for several new classes of experiments on the lunar surface and in lunar orbit that will both provide real-time awareness of space weather conditions during manned missions and advance the field of heliophysics science.

Imaging Type-II emission from a coronal mass ejection with ROLSS would show us where acceleration is occurring, allowing us to determine the coronal conditions that lead to efficient particle acceleration. Observations from the array could also be used in real-time to indicate when a coronal mass ejection has begun to produce radiation. This capability could provide advance warning for astronauts in deep space that a radiation event is imminent, buying valuable time for them to seek shelter. LUNAR Heliophysics team members are involved in other NASA projects related to astronaut safety and the lunar and deep-space radiation environments. LUNAR Co-I Kasper is also a Co-I on the Cosmic Ray Telescope for the Effects of Radiation (CRaTER) on the Lunar Reconnaissance Orbiter (LRO) spacecraft, which has been in a lunar polar orbit for almost three years (Spence et al., 2010). CRaTER is capable of making detailed measurments of the radiation environment and dose (e.g. Schwadron et al, 2012), but is also contains a simple 35 gram micro-dosimeter on a chip (Mazur, et al, 2011). As solar activity increases, the Heliophysics team will be able to quantitatively evaluate the relative value for human spaceflight of advance warnings of radiation from a radio array vs simple and sophisticated radiation measurements at the moon.

## 2. Lunar Radio Observatory Design and Deployment

Project Leaders: Dr. Robert MacDowall, NASA Goddard Space Flight Center
Dr. Joseph Lazio, Jet Propulsion Laboratory
Dr. Justin Kasper, Harvard-Smithsonian Center for Astrophysics

a. *The Radio Observatory on the Lunar Surface for Solar studies (ROLSS) Concept*

Although low-density plasmas make up the majority of the solar system and universe, they have never been imaged at high resolution. The Radio Observatory on the Lunar Surface for Solar studies (ROLSS) is a concept designed to provide the first images of the inner solar system at wavelengths longer than those penetrating the terrestrial ionosphere (~30 m). Its key science target is to localize particle acceleration caused by shocks and reconnection in the inner heliosphere, using solar radio burst emission as the "observable", addressing NASA Strategic Goal 2.2 ("Understand the Sun and its interaction with Earth and the solar system"). ROLSS will

also measure the temporal and spatial variability of the lunar ionosphere and detect interplanetary and interstellar dust striking the antennas.

The ROLSS concept (Figure 4) consists of 3 arms of thin polyimide film (PF), each 500 m in length, radiating from a central hub, providing ~2º angular resolution at 30-m wavelength (10 MHz). The system is located near the lunar equator on the near side. Each arm includes 16 dipole antennas, consisting of metal deposited on the film and the transmission lines connecting them to receivers at the central hub. These arms could be deployed using a crewed or robotic rover. The data collected by the antennas are processed at the central hub and down-linked to Earth for final radio image synthesis. This antenna system is uniquely suited to the low mass and low volume requirements for delivery to the lunar surface.
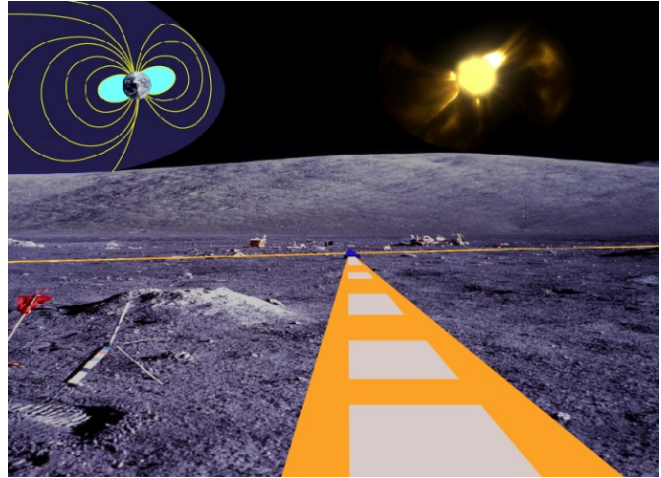
Fig.4 - The arm extending towards the reader shows wide linear dipoles on Kapton®. The other two arms are barely visible in the distance. ROLSS could be the first mission to image the sun and celestial sphere at 1-10 MHz. (Artist's concept of ROLSS array on lunar surface.)

The array operates over the wavelength range 30–300 m (1–10 MHz), with a selectable, variable frequency sub-band that can be placed anywhere within the operational wavelength range. During the course of the concept study, the NASA/GSFC Instrument Design Laboratory (IDL) provided an intensive engineering study of the ROLSS concept. We refer to the conclusions of this study as output from the "IDL run."

Table 1 – Summary of ROLSS Parameters		
Parameter	**Value**	**Comment**
Wavelength (Frequency)	30–300 m (1–10 MHz)	• Matched to radio emission generated by particle acceleration in the inner heliosphere • Obtain spectra of Galactic and extragalactic sources at longest wavelengths • Probe lunar ionosphere • Operate longward of Earth's ionospheric cutoff
Angular Resolution	2º (@10 MHz 20º (@1 MHz	• Localize particle acceleration sites in CMEs and Type III solar bursts • Order of magnitude improvement
Bandwidth	100 kHz	Track temporal evolution of particle acceleration
Lifetime	1 yr	Obtain measurements during several solar rotations

Figure 5a shows a nominal layout of 16 science antennas along each arm. Standard radio astronomical software within the Astronomical Image Processing Software (AIPS) package of the National Radio Astronomy Observatory (NRAO) was used to simulate the instantaneous or "snapshot" point spread function (PSF) or "beam" of the ROLSS array, assuming 16 antennas on each arm and logarithmic spacing along the arm. The 6-arm "star" pattern of the beam in Figure 5b reflects the Y shape of the ROLSS array. The dynamic range in the beam—defined as the ratio between the peak and the rms level—is 15 dB. This dynamic range is consistent with a simple estimate that the rms level in an interferometric image should be of order $1/N$ if the array consists of N antennas. For $N \sim 50$ ($\sim 16 \times 3$), the expected rms level is 2% (-17 dB) of the peak.

b. *The end-to-end ROLSS observing system*

The ROLSS array consists of multiple science antennas. Each science antenna is a single polarization, electrically short dipole, deposited on a PF; also deposited on the PF are the transmission leads to the CEP. The PF is flexible enough to be stored in a roll during transit and deployed directly on the lunar surface by unrolling.

We have conducted two tests of the ROLSS antenna concept. The first test was a comparison of the feed point impedance of a PF antenna lying directly on the ground. This test was conducted by NRL to verify that simulations of the antenna concept were accurate and did not involve extrapolations of modeling software into a regime of parameter space for which they are not valid. The agreement between the simulations and measurements was considerable (Figure 5; Lazio et al. 2011). The second test, carried out by U. Colorado, was to expose the PF to UV radiation and temperature swings characteristic of what the lunar surface experiences. The PF appears to be robust under lunar environmental conditions (Lazio et al. 2011).
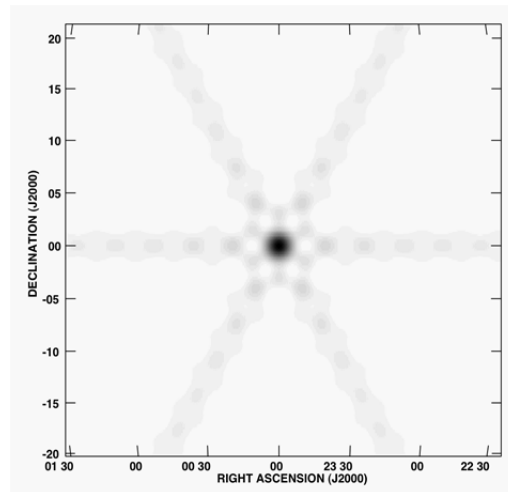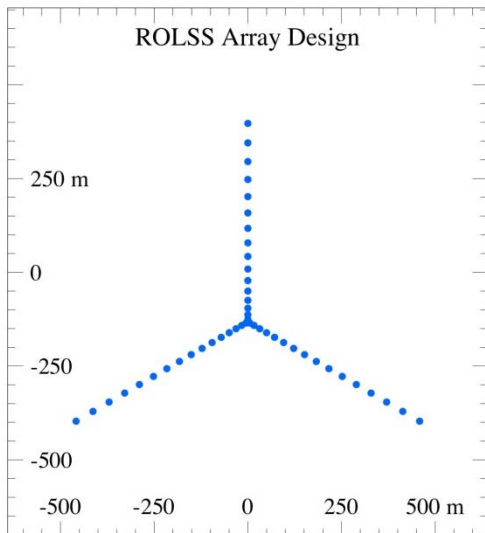

Fig. 5a – (Left) Nominal science antenna distribution along the antenna arms. **Fig. 5b** – (Right) The resulting point-spread function ("beam") for a snapshot image. The maximum sidelobe is at −5.9 dB and the rms sidelobe level is −15 dB, sufficient to achieve ROLSS goals.

Transmission lines carry the signals from the antennas to the CEP. Like the antennas, they consist of a conductor deposited on the PF. Each transmission line is a coplanar waveguide structure (62 mm wide). Simulations, conducted as part of the IDL run, indicate that the gap between the lines reduces cross coupling and suggest that the lines should be placed symmetrically to reduce antenna pattern distortions. These simulations suggest that ~25 dB of signal loss will occur on the longest transmission lines, which must be compensated for at the receiver. Investigation of using active elements on the PF and alternate signal transmission line designs is ongoing.

The width of the transmission lines is determined in part by the requirement of mitigating micrometeorite damage. The estimated bombardment rate at the Moon's surface is 4.9 m^{-2} yr^{-1} for impacts producing craters up to 1 mm wide. Larger craters are sufficiently rare that none were seen in a 3.6-yr exposure. The longest transmission lines are likely to receive a few impacts per year (~ 3), but none are likely to be so large that the transmission line will be completely severed. As with any radio array, ROLSS is robust against the loss of a subset of antennas.
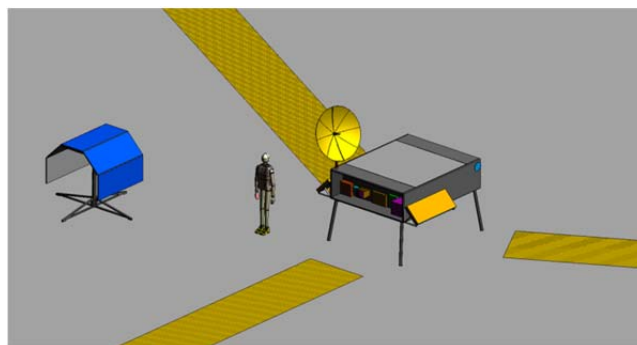
Fig. 6 – ROLSS Central Electronics Package (CEP) showing relative sizes of electronics box with thermal louvers, high-gain antenna, and solar arrays. (Figure from IDL run.)

The ROLSS CEP (shown in Figure 6) houses all of the science antenna receivers including preamplification, data acquisition hardware, power supply electronics, data and telemetry communications electronics, and the thermal management system for these components. The CEP is designed to be carried in a single lunar lander carrier. When deployed, the CEP stands ~1 m above the lunar surface in order that the thermal management system is not subject to dust contamination.

ROLSS uplink telemetry and commanding would be handled by an S-band uplink. A nominal configuration has a 9-m diameter or larger antenna at a site such as GSFC Wallops. The ROLSS CEP would contain an S-band transceiver, which could also be used for data downlink in emergency situations. Data downlink would be handled by a Ka-band system. The ROLSS CEP would host a 0.6-m diameter parabolic gimbaled antenna. The conclusion of the IDL run was that a Ka-band downlink via such an antenna provided the current optimum based on downlink data requirements, weather (rain) conditions, and likely ground-station antenna availability.

The ROLSS mission concept calls for lunar day operations only, when solar arrays provide adequate power, i.e., there are no planned nighttime operations. Thermal management is a key requirement for lunar-based instrument-ation. The CEP is equipped with radiators in order to maintain the internal electronics at a temperature below their assumed maximum operating temperature (80º C).

c. *Siting and deployment*

The prime science mission for ROLSS is solar observations, which favor an equatorial site. A near polar site would require that one or more arms of ROLSS be longer than the nominal 500 m length to compensate for the foreshortening of the arm and maintain the same angular resolution.
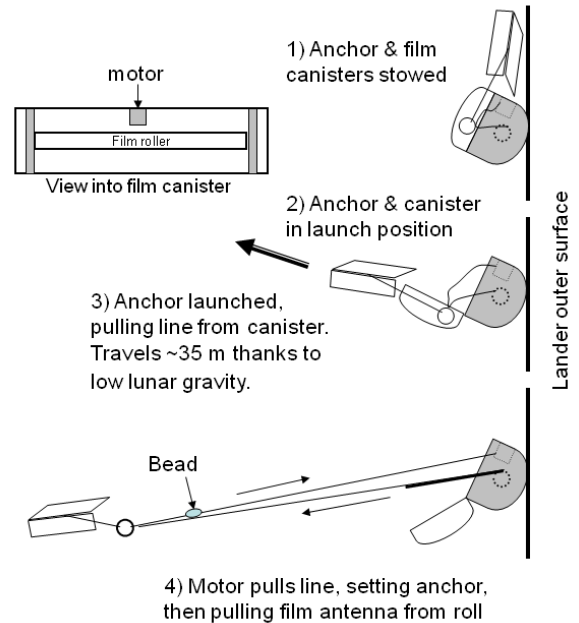
The site itself should be of relatively low relief topography (e.g., the surface of a *mare* vs. the highlands). The entire site does not have to be flat as the fraction of the area occupied by the antenna arms is relatively small—for a circular area with a radius of 500 m, the antenna arms occupy only 0.3% of the total area. Further, there is no requirement on the absolute orientation of the arms. Rotating the arms about the center of the array merely rotates the beam pattern on the sky. The *relative* orientation of the arms is required to be 120º ± 6º, with the error determined by requiring that the nominal antenna position not vary by more than 1 wavelength at the extreme end of an arm. Only modest requirements are set on the smoothness of the antenna arm locations. The shortest operational wavelength for ROLSS would be λ = 30 m, and an individual science antenna would be 15 m in length. Requiring that the antenna

Fig. 7 – ROLSS Precursor (ROLSS-P) deploys ~50 m of film from side of lander.

Fig. 8 – Artist's concept of ROLLS-P pathfinder.

shapes are not distorted by more than $\lambda/10$ implies that deployment requires linear extents of order 500 m with elevation variations not larger than ~3 meters along the intended antenna arm positions. We assume that on the timescale of likely deployment for ROLSS that any site will have better than meter-scale resolution images available (post-Lunar Reconnaissance Orbiter).
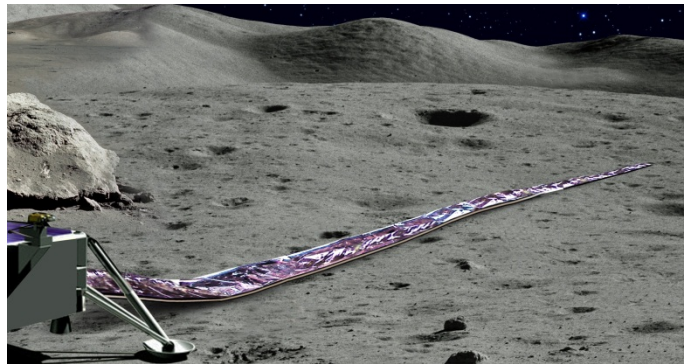
The ROLSS deployment itself could be done completely robotically, by astronauts on a crewed rover, or with a mix of these two modes. Scaling from JPL's ATHLETE rover, a ROLSS rover could be designed to carry and deploy tens of kilograms of antenna mass.

c. *A Pathfinder for ROLSS*

ROLSS is sufficiently complex that prudent management suggests a smaller, lower cost pathfinder needs to land on the moon first. We anticipate that a single length of PF of less than 50 m with ~2 antennas would be the right size for this pathfinder. Such a short length of film

could be launched from a box mounted on the side of a lunar lander, as suggested by Figure 7. This deployer, using a spring-launched anchor to hold the pulley for a line that would pull out the film as shown in the artist's concept (Figure 8), is currently being designed and developed at GSFC.

3. Measuring Interplanetary Dust Impacts on the Lunar Surface with a Radio Array

Project Leader: Dr. Justin Kasper, Harvard-Smithsonian Center for Astrophysics

Interplanetary space is pervaded by dust with sizes ranging from nanometers to tens of microns and larger. Recent work on interplanetary dust has revealed a substantial population of nanometer size dust, or nanodust, with fluxes hundreds of thousands of times higher than better understood micron-sized dust grains. This nanodust tends to move with the speed of the solar wind, or at hundreds of kilometers per second, as opposed to more typical Keplerian speeds of tens of kilometers per second. Since impact damage grows faster than the square of the impact speed for high speed dust, this nanodust can generate significant damage when it impacts an object such as a spacecraft, or a planet, or a moon, as shown in Figure 9. In this section we describe how a low frequency radio array is ideal for measuring the distribution of dust particles as a function of size in interplanetary space, and ultimately for understanding how dust modifies the surfaces of planets and other objects in the solar system.

Dust has many sources, including collisions between asteroids, escaping gas from comets, and condensation within the solar atmosphere. Additional dust streams into the solar system from interstellar space. The size, speed, and mass distribution of dust in interplanetary space and its variation with time tell us about the history of these sources. Measurements of dust properties have been performed with dedicated dust instruments specifically designed to characterize dust particles (Grun et al., 1993; Srama et al., 2004). More recently, it has been shown that space-based radio receivers can also be used to measure dust. These radio instruments function by measuring the electrical signals produced when dust grains impact objects at high speed and create expanding clouds of plasma (e.g. Meyer-Vernet, 2001, Zaslavsky et al. 2012, and references therein). Work on the use of radio receivers for studying dust, including recent results supported by NLSI/LUNAR, have shown that radio observations have two particular strengths when it comes to conducting a survey of the interplanetary dust population. First, radio arrays are very sensitive to nanodust, a major fraction of the dust population in the solar system that produces weak signals in standard instruments. Second, a radio array is also ideal for searching for the highest mass, but rarest dust particles, because the entire surface area of the array, which for lunar concepts exceeds thousands of square meters, becomes a single sensitive dust detector.
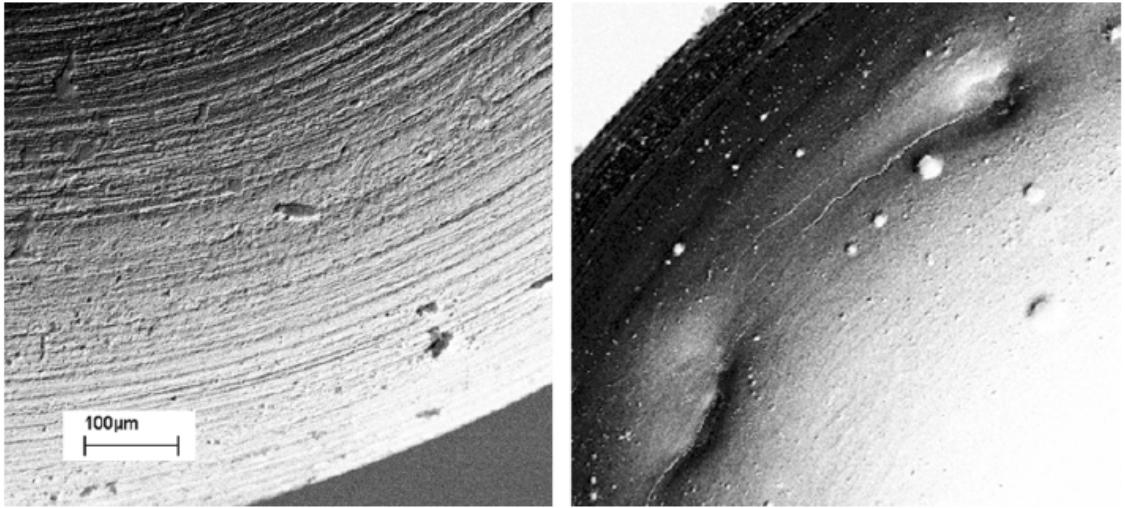
Fig. 9 - Electron microscope images of a target before (left) and after (right) being exposed to high speed dust impacts. If 1 μm dust impacts a target at 20 km/s it produces a 50 micron diameter crater. 10 nm dust is much smaller, but since it moves at 300 km/s, it can create a 1 micron crater, and is much more common than larger dust grains.

Recently, Meyer-Vernet et al. (2009) proposed that small signals seen by the electric field antennas one the STEREO spacecraft may be due to nano-meter scale dust particles. In order to determine the range of masses, and the uniqueness of radio measurements of dust properties, the NLSI/LUNAR/Heliophysics team analyzed dust impacts recorded by the STEREO/WAVES radio instrument onboard the two STEREO spacecraft near 1 AU during the period 2007-2010. The objective of this work was to develop an analytic set of equations to describe the evolution of a plasma plume created when dust strikes an object such as an electric field antenna, and to use these resulting equations to derive the mass distribution of the dust observed by STEREO. These results are in press (Zaslavsky et al., 2011), and were presented at 2010 American Geophysical Union and the 2011 Lunar Science Forum.

The impact of a dust particle on a spacecraft produces a plasma cloud whose associated electric field can be detected by on-board electric antennas, as shown in Figure 10. In our study, we used the electric potential time series recorded by the waveform sampler of the instrument. The high time resolution and long sampling times of this measurement enabled us to deduce considerably more information than in previous studies based on the dynamic power spectra provided by the same instrument or by radio instruments onboard other spacecraft. The large detection area compared to conventional dust detectors provides flux data with a better statistics. Both of these improvements on previous studies would continue with the use of a larger lunar array.
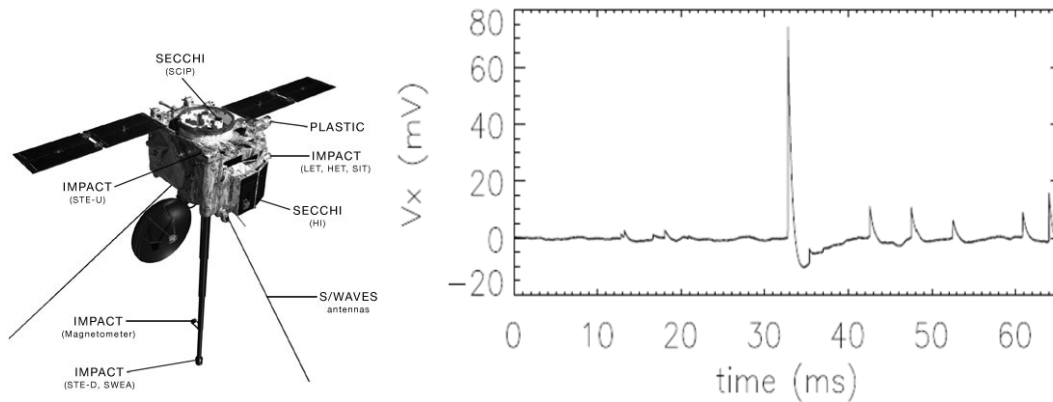
Fig. 10 - The LUNAR Heliophysics Key Project has made use of observations by the electric field antennas on the twin STEREO spacecraft (**one of which is shown on the** left) to examine the radio signatures of dust impacts. Sudden changes to the spacecraft potential as measured by individual antennas (right) are produced when an interplanetary dust particle impacts the spacecraft. Since the antennas are detecting the large scale plasma plume produced by a dust impact, they are sensitive to impacts over many square meters or surface area, and therefore are capable of conducting high sensitivity searches for rare impacts.
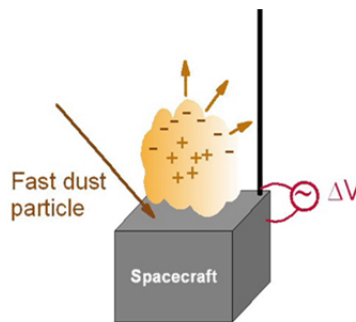

Fig. 11 - Creation of an expanding cloud of plasma surrounding a spacecraft after the impact of a dust grain. Since ions and electrons in the cloud have the same thermal energy, the electrons expand much more quickly.

The process responsible for the signal seen by a radio antenna near the impact of a dust grain is shown in Figure 11. When a grain impacts an object at extremely high speeds (a hyperkinetic impact), it generates a cloud of high temperature plasma of total charge approximately proportional to the mass of the grain and the speed of the grain to the 3.5 power. Since ions and electrons in the cloud have the same thermal energy, the electrons expand much more quickly, and create a large potential drop along the antenna. Our analysis suggests that this technique works very well for measurements that cover the mass intervals $10^{-22} - 10^{-20}$ kg and $10^{-17} - 5 \times 10^{-16}$ kg. The flux of the larger dust agrees with measurements of other instruments on different spacecraft, and the flux of the smaller dust grains agrees with theoretical predictions. Figure 12 shows the variation of the dust flux in a given dust range as a function of time. Figure 13 shows a summary of the typical dust fluxes as a function of mass. For a lunar radio array with 3 arms of 500 m length each and average antenna width on the arms of 1 m, the surface area would be 1500 m^2. Given the flux distribution measured in Figure 13, this would correspond to

approximately 10^3 dust impacts per second for nanodust, and detections of the heavy 10 micron dust several times a minute.
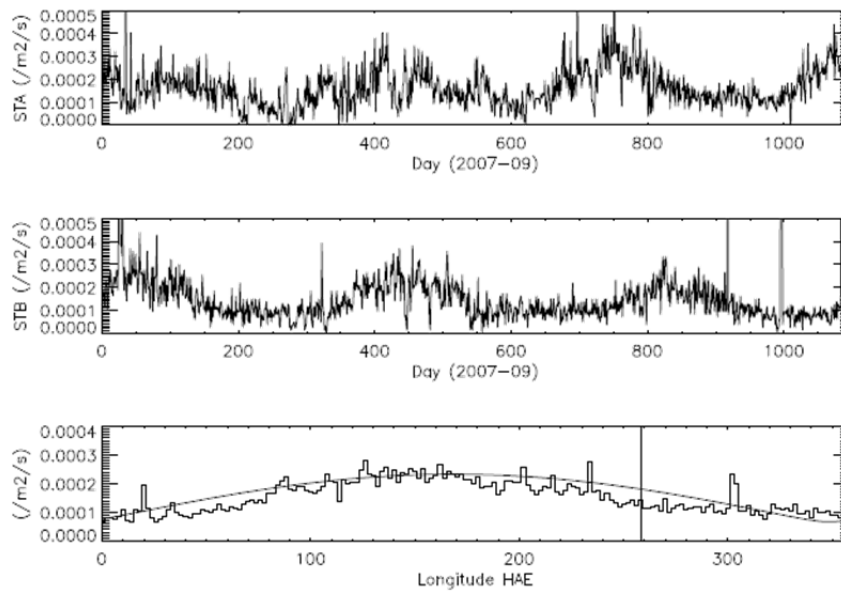
Fig. 12 - The top panel shows the flux of 0.1-0.3 μm dust grains as observed by the STEREO-A and STEREO-B spacecraft respectively, over the course of several years, showing an average flux of about 10^{-4} grains/m²/s. Both spacecraft see a constant term, which is the uniform interplanetary component of the micron-sized dust, along with a modulated component with a one year period. The modulated component is a steady stream of interstellar dust flowing into the solar system in the direction of the Sun's motion through the galaxy. The lower panel shows the dust rates observed by the two spacecraft as a function of longitude in the Heliocentric Aries ecliptic coordinate system, illustrating how the changing orbital velocity vector of the spacecraft orbiting the Sun combines with the velocity of the solar system in interstellar space to modulate the rate of interstellar dust impacts.
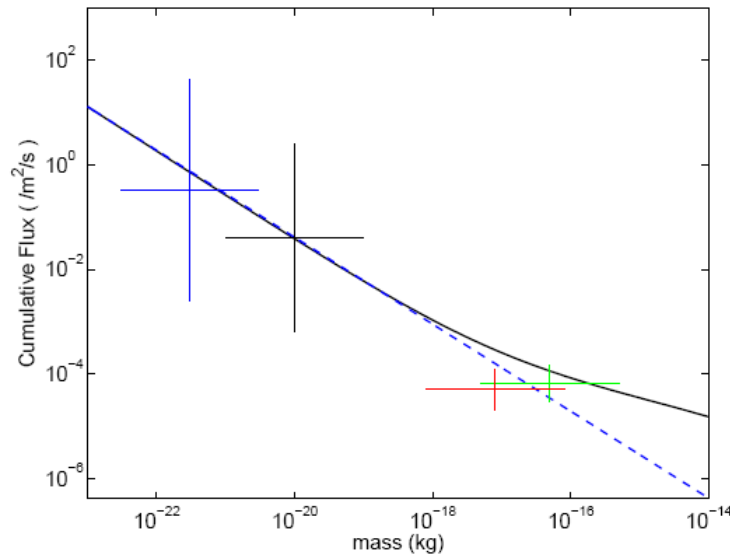
Fig. 13 - Comparison between the dust fluxes as a function of mass as determined though our analysis of the STEREO/WAVES radio observations (symbols) and an equilibrium model of interplanetary dust (solid and dashed lines, Grun et al, 1985).

14

Bibliography

Bale, S. D., Reiner, M. J., Bougeret, J.-L., et al. 1999, "The source region of an interplanetary type II radio burst," Geophys. Res. Lett. 26, 1573

Cane, H. V., Erickson, W. C., & Prestage, N. P. 2002, "Solar flares, type III radio bursts, coronal mass ejections, and energetic particles," J. Geophys. Res. (Space Physics), 107, 1315

Gopalswamy, N., Yashiro, S., Kaiser, M. L., Howard, R. A., & Bougeret, J.-L. 2001, "Radio Signatures of Coronal Mass Ejection Interaction: Coronal Mass Ejection Cannibalism?" Astrophys. J., 548, L91

Gopalswamy, N., Yashiro, S., Kaiser, M. L., Howard, R. A., Bougeret, J.-L. 2002, "Interplanetary radio emission due to interaction between two coronal mass ejections," Geophys. Res. Lett., 29, 080000-1

Gopalswamy, N., Yashiro, S., Krucker, S., Stenborg, G., & Howard, R. A. 2004, "Intensity variation of large solar energetic particle events associated with coronal mass ejections," J. Geophys. Res. (Space Physics), 109, 12105

Grun et al. 1985, "Collisional balance of the meteoritic complex", Icarus 62, 244-272

Grun et al 1993, "Discovery of Jovian dust streams and interstellar grains by the Ulysses spacecraft", Nature 362, 428 - 430 (01 April 1993); doi:10.1038/362428a0

Lara, A., Gopalswamy, N., Nunes, S., Muñoz, G., & Yashiro, S. 2003, "A statistical study of CMEs associated with metric type II bursts," Geophys. Res. Lett., 30, 120000-1

Lazio, T. J. W., MacDowall, R. J., Burns, J. O., et al. 2011, "The Radio Observatory for Lunar Surface Solar Studies," Adv. Space Res., in press

MacDowall, R. J., Bale, S. D., Demaio, L., et al. 2005, "Solar Imaging Radio Array (SIRA): A Multispacecraft Mission," in Enabling Sensor and Platform Technologies for Spaceborne Remote Sensing: Proceedings of the SPIE—Volume 5659, eds. G. J. Komar, J. Wang, & T.

Mazur, J. E., et al., 2011, Space Weather, 9, S07002, doi:10.1029/2010SW000641, New measurements of total ionizing dose in the lunar environment.

Meyer-Vernet, N., 2001. Detecting dust with electric sensors in planetary rings, comets and interplanetary space. ESA SP-476 (Edited by R. A. Harris), 635640.

Meyer-Vernet, N., et al. 2009, "Dust detection by the wave instrument on stereo: nanoparticles picked up by the solar wind?", Solar Physics 256, 463–474.

Oberoi, D. et al., 2011, Astrophys. J. Lett., 728, 2, L27, doi:10.1088/2041-8205/728/2/L27, First Spectroscopic Imaging Observations of the Sun at Low Radio Frequencies with the

Murchison Widefield Array Prototype

Schwadron, N. A., et al., 2012, J. Geophys. Res., 117, E00H13, doi:10.1029/2011JE003978, Lunar radiation environment and space weathering from the Cosmic Ray Telescope for the Effects of Radiation (CRaTER)

Spence, H. E., et al., 2010, Space Science Reviews, doi:10.1007/s11214-009-9584-8, CRaTER: The Cosmic Ray Telescope for the Effects of Radiation Experiment on the Lunar Reconnaissance Orbiter Mission

Zaslavsky et al 2011, "Interplanetary dust detection by radio antennas: mass calibration and fuxes measured by STEREO/WAVES", Journal of Geophysical Research - Space Physics, accepted, in press..